HHS Public Access

Author manuscript

Ocul Surf. Author manuscript; available in PMC 2021 October 01.

Published in final edited form as:

Ocul Surf. 2020 October ; 18(4): 821–828. doi:10.1016/j.jtos.2020.07.021.

The impact of euthanasia and enucleation on mouse corneal epithelial axon density and nerve terminal morphology

Gauri Tadvalkar, Ph.D.[1], **Sonali Pal-Ghosh, MS**[1], **Ahdeah Pajoohesh-Ganji, Ph.D.**[1], **Mary Ann Stepp, Ph.D.**[1,2,*]

[1]Department of Anatomy and Cell Biology, The George Washington School of Medicine and Health Sciences, Washington DC 20037

[2]Department of Ophthalmology, The George Washington School of Medicine and Health Sciences, Washington DC 20037

Abstract

Introduction: Here we study the impact of using either CO_2 gas or cervical dislocation (CD) for euthanasia and using different techniques to enucleate the eye on preserving axonal density and morphology of the intraepithelial corneal nerves (ICNs).

Objectives: To determine whether using CO_2 gas or CD for euthanasia and enucleating by cutting or pulling eyes out impacts axon density and nerve terminal morphology in the mouse cornea.

Methods: Mice were euthanized by CO_2 gas or CD; the impact of delaying fixation for 5 minutes post-euthanasia was also assessed. We tested two different techniques to enucleate the eyes: cutting the optic nerve by curved scissors or pulling the eye out. A minimum of 10 corneas from 5 male and female BALB/c mice were used for each variable. Axons and intraepithelial corneal nerve terminals (ICNTs) were visualized utilizing βIII tubulin and L1CAM and quantified using confocal microscopy.

Results: The variations seen in axon density between individual mice are not gender- or euthanasia-dependent. A significant reduction in axon density and loss of ICNT morphology are observed in eyes enucleated by pulling the optic nerve out. Similar results are obtained in male and female mice.

Conclusion: While the variations tested in euthanasia do not affect axon density in male and female mouse corneas, enucleation by proptosing and gently cutting out the eyes yields increased axon density and improved ICNT morphology compared to pulling eyes out and leaving the optic nerve attached.

[*]**Corresponding author:** Mary Ann Stepp Ph.D. Department of Anatomy and Cell Biology, The George Washington School of Medicine and Health Sciences, 2300 I St. NW, Washington DC 20037. (phone) 1-202-994-0557; (fax) 1-202-994-8885 mastepp@gwu.edu.

The authors have no financial or personal relationships that could cause a conflict of interest regarding this article.

Keywords

cornea; axon density; mouse; euthanasia; enucleation

Introduction

Mice are typically euthanized using CO_2 gas, cervical dislocation (CD), or isoflurane gas followed by CD. CO_2 gas can stimulate corneal sensory nerves [1] and cause aversive behavior in rodents [2–5]. Accumulation of CO_2 under contact lenses leads to discomfort due, in part, to reduced pH in the tears and to corneal swelling [6, 7]. We hypothesized that differences in CO_2 exposure and the length of time between sacrifice and tissue fixation may lead to changes in the pH of the ocular surface. The intraepithelial corneal nerves (ICNs) consist of intraepithelial corneal basal nerves (ICBNs) and intraepithelial corneal nerve terminals (ICNTs). These nerves are thin and if triggered to release vesicles containing neurotransmitters, the ICNs will lose volume and become harder to visualize. Studies using capsaicin in rat corneas by Hegarty and colleagues [8] have shown that topical capsaicin treatment induced neurotransmitter release from sensory axons and reduced axon density; the earliest time point they assessed was 3 hours after treatment.

We have published several studies showing differences in ICNs in dry eye, aging, genetically engineered mice, and after different types of corneal wounds [9–14]. We, like others, have found that ICN density can vary between individual mice and we suspected that differences in euthanasia and tissue harvesting contribute to this variation. This led us to test whether the variation we see in axon density between corneas is inherent between individual corneas or due to the methods used to euthanize mice and collect the eyes.

Our routine procedure involves proptosing the eye and cutting it out using curved scissors. We separate the cornea from the retina after the eye has been fixed overnight. An alternative method to enucleate the eye is to proptose the eye and place a forcep or curved scissor under the eye and pull the eye out; this method is described in detail in the *J. of Visualized Experiments* by Mahajan and colleagues [15]. This procedure results in the optic nerve remaining attached to the back of the eye.

The sensory nerves that innervate the cornea derive from long ciliary nerves whose cell bodies are located in the ophthalmic branch of the trigeminal ganglion [16]. The long ciliary nerves located along the outside of the optic nerve penetrate the eye along with the optic nerve at the Annulus of Zinn. The ciliary nerves extend towards the anterior segment and limbus where they enter the corneal stroma and, from there, the epithelium [17]. When the eye is pulled out, the long ciliary nerves stretch until they sever. We speculate that cutting the eye out with scissors places less mechanical force on the long ciliary nerves than pulling the eye out until they mechanically sever. These forces could induce protease activation and/or the release of secretory vesicles by the sensory nerves and affect the nerve density analysis.

Methods:

Animals:

All studies performed comply with The George Washington University Medical Center Institutional Animal Care and Use Committee guidelines and with the ARVO Statement for the Use of Animals in Ophthalmic and Vision Research. For these studies, 7 to 8-week old male and female BALB/cN mice were used. Six different variations of euthanasia were assessed: **1. Standard Of Care (SOC)** euthanizing with CO_2 at 3 LPM until breathing stops (approximately 3.0 – 3.5 minutes), **2. SOC+5** euthanizing with SOC and leaving mice in the cage with the CO_2 gas turned off for an additional 5 minutes, **3. Cervical Dislocation (CD)** euthanizing mice with cervical dislocation, **4. CD+5** euthanizing with cervical dislocation and waiting 5 minutes before enucleating and placing the eyes in fix, **5. ISO+CD** using isoflurane gas until mice are unconscious (30 seconds - 1.0 minute) followed by CD, and finally **6. ISO+5+CD** mice are left in the isoflurane chamber for an additional 5 minutes followed by CD. Eyes were placed immediately into fix as described in the methods section. All variables had 5 mice per cage.

The two different methods of enucleation assessed were removal of the proptosed eyes using curved scissors (optic nerve cut, ONC) and pulling the eye out using a curved scissor leaving the optic nerve attached to the posterior aspect of the globe (optic nerve pull, ONP). To prevent sensory axons from firing while the eyes were being enucleated, we also applied a drop of proparacaine to the ocular surface after euthanasia and waited for one minute prior to enucleation.

Immunofluorescence:

All eyes were fixed immediately after enucleation in a paraformaldehyde-containing fixative (1x PBS, 1% formaldehyde, 2-mM MgCl2, 5-mM EGTA, 0.02% NP-40) for 1 hour and 15 minutes at 4°C, followed by two washes for 10 minutes each in 1x PBS containing 0.02% NP40 at room temperature. Tissues were then placed in 4:1 methanol:dimethyl sulfoxide (DMSO) for 2 hours at −20°C and then stored in 100% methanol at −20°C until used for whole-mount staining studies. The back of the eye was cut and the retina, lens, and iris removed before staining. Tissues were transferred to a graded Methanol-TritonX-100 series (75%, 50%, and 25% methanol: TritonX-100 for 15, 15, and 10 minutes, respectively). All incubations were performed with gentle shaking and at room temperature, unless otherwise specified. The eyes were washed twice in PBS, for 30 minutes each, followed by incubation with blocking buffer for 2 hours. Blocking buffer was made as follows: to 100 mL 1x PBS, 1 g of BSA was added, the mixture was stirred for 10 minutes, 1 mL of horse serum was added, and the mixture was stirred for an additional minute.

The tissues were then incubated overnight with primary antibody diluted in blocking buffer at 4°C. Sensory axons are visualized using antibodies against βIII tubulin (TUJ1; #801201; Biolegend) and L1CAM (#MAB5272; Millipore). L1CAM is an integral membrane cell adhesion protein present on axon surfaces. To assess cell proliferation, an antibody against ki67 (#ab16667; Abcam) was used. Appropriate secondary DyLite 488 and 594 antibodies from Jackson Immunobiologicals (West Grove, PA, USA) were used for immunolabeling.

The next day, the tissues were washed five times with PBS and 0.02% Tween 20 (PBST) for 1 hour each, blocked for 2 hours, and then incubated with secondary antibody diluted in blocking buffer overnight at 4°C. The following day, eyes were washed three time with PBST for 1 hour each, followed by nuclear staining with 4,6-diamidino-2- phenylindole (DAPI) for 5 minutes, and washed with distilled water. To achieve the best flattening, the corneas were placed epithelial side-up with Fluoromount G mounting media (#17984–25; Electron Microscopy Sciences) and coverslipped.

Confocal microscopy:

Confocal microscopy was performed at the GW Nanofabrication and Imaging Center at The George Washington University Medical Center. A confocal laser-scanning microscope (Zeiss 710; Carl Zeiss, Inc.) was used to image the localization of Alexa Fluor 488 (argon laser; 488-nm laser line excitation; 495/562 emission filter; Jackson Immunobiologicals), and Alexa Fluor 594 (561 diode laser; 594-nm laser line excitation; 601/649 emission filter; Jackson Immunobiologicals). Optical sections (z = 0.5 μm) were acquired sequentially with a 63x objective lens. Three-dimensional (3D) images were rotated to generate cross section views using Volocity software (Version 6.3; Perkin Elmer, New York, NY, USA). High-resolution images were presented either as cross sections projected through the length of the acquired image (135 μm), or as cross-sections projected through 0.5 μm of tissue. Image J was used for the measurement of the lengths of apical axons and Neuron J for the stromal nerve quantitation. Each image subjected to quantification was obtained using the same confocal laser settings and the same intensity settings in Volocity to permit valid comparisons.

For Sholl and stromal nerve analyses, images were acquired using the Zeiss Cell Observer Z1 spinning disk confocal microscope (Carl Zeiss, Inc., Thornwood, NY, USA), equipped with ASI MS-2000 (Applied Scientific Instrumentation, Eugene, OR, USA) scanning stage with z-galvo motor, and Yokogawa CSU-X1 spinning disk. A multi-immersion 25x/0.8 objective lens, LCI Plan-Neofluor, was used for imaging, with oil immersion. Evolve Delta (Photometrics, Tucson, AZ, USA) 512 × 512 EM-CCD camera was used as detector (80-msec exposure time). A diode laser emitting at 568 nm was used for excitation (54% power). Zen Blue software (Carl Zeiss, Inc.) was used to acquire the images, fuse the adjacent tiles, and produce maximum intensity projections. The adjacent image tiles were captured with overlap to ensure proper tiling. All images were acquired using the same intensity settings. To allow quantification of ICNs and stromal nerves, confocal images stacks at two different depths were obtained for each cornea assessed.

Sholl analysis was performed using ImageJ as described previously [18]. Sholl analysis yields data on the number of times an axon crosses each radius in the target. The radii range from 5–75 μm and are 5 μm part; there are a total of 15 radii assessed per target. Image J determines the number of times an axon intersects each radius in the target; the total number of intersections is divided by the total number of radii per target (15). There are 7 targets overall (4 peripheral and 3 central); the average number of interactions per target is then determined. We use the term “axon density” to indicate the average number of intersections per target for each cornea assessed.

For measuring the length of the stromal nerves, we used Neuron J as follows: We loaded Neuron J (through Image J), opened each stromal nerve image, converted the image to 8 bit and saved it as a jpg. We used the 'Add tracing' tool from the tool bar to draw along the length of the nerve. We then double clicked to end tracing of each stromal nerve. We used 'Measure tracing tool' to determine the length of the nerve in μm.

For cell proliferation studies, images were acquired on the Nikon E600 Fluorescent Microscope and the numbers of ki67+ cells per field were analyzed using ImageJ. 2 fields were imaged in each peripheral zone (4 zones) and 2 images at the corneal center, so 10 fields total per eye were assessed.

Statistical analyses:

Quantitative data are presented as mean ± standard error of the mean. The number of corneas used for each assessment are indicated on each figure. All statistical tests were performed using the GraphPad Prism Program, Version 6 (GraphPad Software, Inc. San Diego, CA). When more than 2 groups are compared and the standard deviations are not significantly different, the parametric one way ANOVA test is used; when more than 2 groups are compared and the standard deviations are significantly different, the non-parametric Kruskal-Wallis is used. When 2 groups are compared and the standard deviations are not significantly different, the parametric unpaired student t test is used; when 2 groups are compared and the standard deviations are significantly different, the non-parametric Mann-Whitney test is used. p values < 0.05 are considered statistically significant.

Results:

ICNs are retained equally well despite variations pre- and post-euthanasia.

A representative flattened projection image acquired using the Zeiss spinning disk microscope showing the ICNs is presented in Figure 1A; this image was acquired by stitching together 3 rows of 7 individual images (21 images). As described previously [18], Sholl analysis involves placing a circle containing several concentric circles on the image and counting the number of times an axon crosses the circles (radii) in each target. Sholl analysis determined the average number of intersections per target. As shown in Figure 1B, each group contains 10 corneas from male mice and no significant differences were found among groups. Combining the SOC and the SOC+5, the CD and CD+5, and the ISO-CD and the ISO-CD+5 groups to yield 3 groups with 20 corneas each does not alter the outcome. Thus, we find no evidence to support the idea that CO_2 exposure or an extra 5 minutes between sacrifice and fixation impacts ICN morphology. As long as eyes are placed in fix within 5 minutes after sacrifice, 5 mice can be euthanized at the same time in a single cage without negatively impacting axon density of their corneas. Even though corneas are not exposed to CO_2 gas and are placed into fix immediately after sacrifice by CD, they do not have higher axon densities than mice sacrificed by SOC. Finally, the variation in axon density seen among corneas of the same group (standard deviations) are not significantly different between groups.

The variation seen in axon density between left and right eyes of individual mice is the same as that seen between mice.

Studies of the mouse cornea, including studies of corneal development and dry eye disease, often involve pathology in both left and right eyes. In such cases, data can be expressed based either on the number of corneas or the number of mice used for the study. We next evaluate whether there is a difference in the variation between axonal density values obtained from the average of values from left and right corneas (n = the number of mice used) compared to each cornea being considered an independent variable (n = the number of corneas used). We use our SOC method to euthanize 10 mice from 2 cages (1 and 2), each cage containing 5 mice. Each mouse was assigned a number and each eye labeled by that number and as left or right. Each cornea was kept separate from all others throughout fixation, processing, staining, and flat mounting. One of the left eyes was either damaged during processing or scarred and was excluded from analysis. We quantify axon density using Sholl analysis.

Data for each cornea are presented in Table 1A along with the means, standard deviations (SDs), and standard errors of the mean (SEMs). The means for the left and right eyes are 21.8 +/− 3.9 (n=9) and 19.3 +/− 3.2 (n=10) arbitrary units. The mean obtained for the left and right eyes averaged together is 20.3 +/− 2.5 (n=9) arbitrary units. While the SD for the group where left and right eyes are averaged together is lower than those for the left and right eyes separately, the difference is not statistically significant. Next, we assessed the data by cage and asked whether considering both left and right eyes of n=5 mice as independent variables is justified. The data from left and right eyes in cage 1 yields a mean of 20.3 +/− 4.6 and cage 2 yields a mean of 20.7+/−2.7. None of these approaches to analyzing the data yields standard deviations that are statistically significantly different by one-way ANOVA. We have previously assessed corneal epithelial cell proliferation and its relationship to axon density in aging and dry eye [12, 13]. We next extend this type of analysis to the measurement of cell proliferation. We assess the numbers of ki67+ cells per field in each of the eyes used to assess axon density and we subjected those data to the same type of analysis presented above for axon density. The results are shown in Table 1B. They also show no significant difference between groups. Thus, these data support the validity of using each cornea as an independent variable when assessing axon density and cell proliferation. Doing so does not reduce the rigor of the analysis and will allow researchers to minimize animal use.

Enucleation method impacts ICN density.

We next compare two different methods of enucleation: ONC and ONP. Representative images for corneas of male and female mice obtained using ONC and ONP used for Sholl analysis are presented in Figure 2A. Quantitative data obtained from Sholl analysis are presented in Figure 2B for axon density in the center of the cornea (areas 5–7 in Fig 1A), at the periphery (areas 1–4 in Fig 1A), and after combining those two data sets to generate a single value for both center and periphery. Data show a significant reduction in axon density in male corneas enucleated by ONP of 30% in the center, 24% in the periphery, and overall 26% compared to ONC. In females, data show a significant reduction in axon density in corneas enucleated by ONP of 9% in the center, 10% in the periphery, and overall 10%

compared to ONC. While the difference in the center of the female corneas enucleated by ONP is not significant compared to ONC, the differences are significant in the periphery and in the data from both central and peripheral corneas. The variation seen between individual female corneas is less than that seen in male corneas; in addition, the variation seen in male ONP corneas is greater compared to the male ONC corneas. Proparacaine applied after sacrifice does not attenuate the effect of nerve pull on axon density suggesting that firing of the ICNs is not a factor in the reduction in their density.

Sholl analysis uses projection images to quantify axon density; this type of imaging favors studying the ICBNs but is not capable of imaging the ICNTs, which extend perpendicular to the epithelial basement membrane. When ICNTs reach the apical squames, the nerve terminals turn and extend parallel to the ocular surface (referred to as parallel ICNTs or pICNTs). We next visualize ICNTs and pICNTs to determine whether optic nerve pull also impacts the nerve terminals. The corneas used above for Sholl analysis had been stained to visualize L1CAM and βIII tubulin. Axonal L1CAM is a surface protein whose extracellular domain can be proteolytically cleaved and shed [19, 20]; its protease cleavage site is typically unavailable. In response to mechanical forces, L1CAM undergoes a conformational change that makes the site available and results in rapid cleavage of the L1CAM extracellular domain by any of several proteases secreted by corneal epithelial cells including ADAM10, ADAM17, and BACE1[15, 21, 22]. Next, we obtained high resolution 3D confocal image stacks for L1CAM as well as for βIII tubulin at the vortex at the center of the cornea; representative images are presented in Figure 3A and quantified in Figures 3B and 3C. Data show that L1CAM is retained on pICNTs and the apical most ICNTs after optic nerve pull. However, at the middle and basal aspects of the epithelium, the ICNTs and ICBNs lose L1CAM relative to βIII tubulin. In addition, the morphology of the ICNTs appears disrupted after ONP compared to ONC.

We next quantify the stromal nerves after ONC and ONP. Data from male and female corneal stromas are shown in Figure 5 and no difference in stromal nerve arborization is observed when we compare ONC and ONP. When the eye is pulled out, the long ciliary nerves are stretched until they sever; the forces applied to the ciliary nerves are also applied to the stromal nerves and the ICNs. While the morphology of the thicker stromal nerves is not disrupted, both ICBNs and ICNTs are negatively impacted by ONP compared to our ONC procedure where we cut the eye out severing the long ciliary nerves before removing the eye.

Discussion

The main objective of this study was to develop a standard protocol to euthanize, enucleate and fix the eyes with the goal of minimizing experimental contributions to the variability seen in axonal density to reduce the numbers of mice needed to determine statistical significance. The variability that remains after we have optimized the methods used will be inherent between individuals. We determined that our SOC technique for euthanasia using CO_2 gas was as equally effective as CD and that as long as eyes were placed in fixative within 5 minutes of euthanasia, axon density is not impacted. We find support for treating left and right corneas of mice as independent variables when assessing axon density and

corneal epithelial cell proliferation. The variation in axon density seen between left and right corneas in mice of the same age and strain is equal to the variation seen between individual corneas. Therefore, it is not advantageous experimentally to generate a single n value by averaging values from the left and right corneas of each mouse. While this is true for axon density and cell proliferation, it might not be the case for other types of assessments. Investigators will need to carry out studies similar to those we have performed here before they can conclude that data from 10 corneas from the left and right eyes of 5 mice provide the same robust data as that from 10 left eyes or 10 right eyes from 10 mice.

This paper is the first study to compare the axon density in the corneas of mice whose eyes were enucleated by pulling compared to cutting the eye out. A JoVE paper was published by Mahajan and colleagues [15] describing a method to remove eyes for high throughput screening. The method described involves using curved forceps to grasp the eye by the connective tissue beneath it and pulling it out. We became concerned that the ONP method may be reducing axon density when we were asked to analyze corneas of various genetically engineered mice whose eyes were sent to us by colleagues and had optic nerves attached.

The results presented here confirm that enucleating by pulling the eye and optic nerve out impacts ICN density in both male and female mice. The difference was more pronounced in male (25%) compared to female (10%) mice. The variation we see in the axon densities of male mice is significantly greater than that seen between female mice. Male mice housed together interact with one another and fight more than female mice; corneas are more likely to be injured and scarred in males compared to females. Prior injury could contribute to differences in variability of axon density we see between males and females. The variation seen in the axon density in our ONC male mice is greater than that seen in female mice consistent with them having had minor injuries prior to sacrifice.

In addition to the reduction in axon density seen by Sholl analysis, ONP also impacted the morphology and localization of L1CAM on the ICBNs and ICNTs. Shedding of L1CAM from axonal surfaces destabilizes the nerves [23]. The reduction we see in L1CAM at the basal aspect of the corneal epithelium appears to result from pulling of the stromal nerves on the ICBNs. L1CAM on axonal surfaces and its shedding has been studied for many years [21–23]. Here we document that L1CAM can be shed from the basal-most ICNs within minutes. We place eyes in fix within 5 minutes of sacrifice; the length of time it takes for fixatives to penetrate the corneal epithelium and stop protease activity is not known but it is likely 10–15 minutes.

To enucleate eyes by ONP, we place curved scissors under the proptosed eye and pull without closing the scissors so that the optic nerve remains attached to the eye; yet, scissors may partially sever the ciliary nerves. This could contribute to increased variation in axon densities between individual corneas after optic nerve pull. Yamaguchi and colleagues [16] and Joubert and colleagues [24] show the anatomical locations of the long ciliary nerves in the mouse eye; the nerves can be visualized outside the optic nerve before they enter the eye. Yamaguchi developed a procedure to surgically axotimize the mouse cornea by displacing the eye, severing the long ciliary nerves, and replacing the eye back into the orbit [16]. Using forceps or curved scissors to pull the eye out, may directly sever one of the long

ciliary nerves depending on the positioning of the forceps and the pressure applied to the back of the eye at the time of enucleation. We predict that severing the long ciliary nerves located on the outside of the optic nerve before pulling the eye out may attenuate the differences reported here.

Because the attached optic nerve is often 4–6 mm long and the mouse eye is approximately 3 mm in diameter, we know that the optic nerve severs behind the orbit when ONP is used. We do not know where within the eye the long ciliary nerves sever when eyes are enucleated by nerve pull. We hypothesize that before they sever, the forces transmitted to the stromal nerves and ICNs in the cornea from the ciliary nerves mechanically stretches and activates proteases that lead to the shedding of L1CAM and disrupt the morphology of the nerve terminals. These forces are greater near the stromal nerves so the changes seen in the ICNs are more profound near the ICBNs.

The differences reported above in ICNs density and ICNT morphology due to enucleation by ONP increase the variability seen in ICNs among individual corneas. Using the ONP method to enucleate eyes to compare axon density in mice that have been subjected to different experimental protocols will require larger numbers of mice to demonstrate significance due to the increased variation seen between individual corneas. In addition, if the pathology the mice are subjected to alters the mechanical properties of the sclera or cornea, removing the eyes by pulling the eye out could lead to differences in axon density due to the enucleation method and not because of the treatment the mice were subjected to or to their genetics.

Acknowledgements:

We would like to thank Anastas Popratiloff, MD/PhD, Director and Lead Scientist, GW Nanofabrication and Imaging Center (OVPR) and Professor of Anatomy (SMHS) and The GW Nanofabrication and Imaging Center for assistance with the confocal imaging. In addition, we would like to thank Beverly Karpinsky-Oakley for help in editing the manuscript. This work was funded by NEI RO1EYE 8512 (MAS).

References

[1]. Chen X, Gallar J, Pozo MA, Baeza M, Belmonte C. CO2 stimulation of the cornea: a comparison between human sensation and nerve activity in polymodal nociceptive afferents of the cat. Eur J Neurosci. 1995;7:1154–63. [PubMed: 7582088]

[2]. Niel L, Kirkden RD, Weary DM. Effects of novelty on rats' responses to CO(2) exposure. Applied Animal Behaviour Science. 2008;111:183–94.

[3]. Niel L, Stewart SA, Weary DA. Effect of flow rate on aversion to gradual-fill carbon dioxide exposure in rats. Applied Animal Behaviour Science. 2008;109:77–84.

[4]. Hwang CK, Iuvone PM. Technical brief: a comparison of two methods of euthanasia on retinal dopamine levels. Mol Vis. 2013;19:1122–4. [PubMed: 23734080]

[5]. Guedes SR, Valentim AM, Antunes LM. Mice aversion to sevoflurane, isoflurane and carbon dioxide using an approach-avoidance task. Applied Animal Behaviour Science. 2017;189:91–7.

[6]. Bonanno JA, Polse KA. Measurement of in vivo human corneal stromal pH: open and closed eyes. Invest Ophthalmol Vis Sci. 1987;28:522–30. [PubMed: 3557865]

[7]. Leung BK, Bonanno JA, Radke CJ. Oxygen-deficient metabolism and corneal edema. Prog Retin Eye Res. 2011;30:471–92. [PubMed: 21820076]

[8]. Hegarty DM, Hermes SM, Yang K, Aicher SA. Select noxious stimuli induce changes on corneal nerve morphology. J Comp Neurol. 2017;525:2019–31. [PubMed: 28213947]

[9]. Pal-Ghosh S, Pajoohesh-Ganji A, Tadvalkar G, Kyne BM, Guo X, Zieske JD, et al. Topical Mitomycin-C enhances subbasal nerve regeneration and reduces erosion frequency in the debridement wounded mouse cornea. Exp Eye Res. 2016;146:361–9. [PubMed: 26332224]

[10]. Pal-Ghosh S, Tadvalkar G, Stepp MA. Alterations in Corneal Sensory Nerves During Homeostasis, Aging, and After Injury in Mice Lacking the Heparan Sulfate Proteoglycan Syndecan-1. Invest Ophthalmol Vis Sci. 2017;58:4959–75. [PubMed: 28973369]

[11]. Stepp MA, Pal-Ghosh S, Tadvalkar G, Li L, Brooks SR, Morasso MI. Molecular basis of Mitomycin C enhanced corneal sensory nerve repair after debridement wounding. Sci Rep. 2018;8:16960. [PubMed: 30446696]

[12]. Stepp MA, Pal-Ghosh S, Tadvalkar G, Williams A, Pflugfelder SC, de Paiva CS. Reduced intraepithelial corneal nerve density and sensitivity accompany desiccating stress and aging in C57BL/6 mice. Exp Eye Res. 2018;169:91–8. [PubMed: 29407221]

[13]. Stepp MA, Pal-Ghosh S, Tadvalkar G, Williams AR, Pflugfelder SC, de Paiva CS. Reduced Corneal Innervation in the CD25 Null Model of Sjogren Syndrome. Int J Mol Sci. 2018;19.

[14]. Pal-Ghosh S, Tadvalkar G, Lieberman VR, Guo X, Zieske JD, Hutcheon A, et al. Transient Mitomycin C-treatment of human corneal epithelial cells and fibroblasts alters cell migration, cytokine secretion, and matrix accumulation. Sci Rep. 2019;9:13905. [PubMed: 31554858]

[15]. Mahajan VB, Skeie JM, Assefnia AH, Mahajan M, Tsang SH. Mouse eye enucleation for remote high-throughput phenotyping. J Vis Exp. 2011.

[16]. Yamaguchi T, Turhan A, Harris DL, Hu K, Pruss H, von Andrian U, et al. Bilateral nerve alterations in a unilateral experimental neurotrophic keratopathy model: a lateral conjunctival approach for trigeminal axotomy. PLoS One. 2013;8:e70908.

[17]. May CA. Morphology of the long and short uveal nerves in the human eye. J Anat. 2004;205:113–20. [PubMed: 15291794]

[18]. Pajoohesh-Ganji A, Pal-Ghosh S, Tadvalkar G, Kyne BM, Saban DR, Stepp MA. Partial denervation of sub-basal axons persists following debridement wounds to the mouse cornea. Lab Invest. 2015;95:1305–18. [PubMed: 26280222]

[19]. Burden-Gulley SM, Pendergast M, Lemmon V. The role of cell adhesion molecule L1 in axonal extension, growth cone motility, and signal transduction. Cell Tissue Res. 1997;290:415–22. [PubMed: 9321705]

[20]. Castellani V, Chedotal A, Schachner M, Faivre-Sarrailh C, Rougon G. Analysis of the L1deficient mouse phenotype reveals cross-talk between Sema3A and L1 signaling pathways in axonal guidance. Neuron. 2000;27:237–49. [PubMed: 10985345]

[21]. Gutwein P, Oleszewski M, Mechtersheimer S, Agmon-Levin N, Krauss K, Altevogt P. Role of Src kinases in the ADAM-mediated release of L1 adhesion molecule from human tumor cells. J Biol Chem. 2000;275:15490–7. [PubMed: 10809781]

[22]. Mechtersheimer S, Gutwein P, Agmon-Levin N, Stoeck A, Oleszewski M, Riedle S, et al. Ectodomain shedding of L1 adhesion molecule promotes cell migration by autocrine binding to integrins. J Cell Biol. 2001;155:661–73. [PubMed: 11706054]

[23]. Maretzky T, Schulte M, Ludwig A, Rose-John S, Blobel C, Hartmann D, et al. L1 is sequentially processed by two differently activated metalloproteases and presenilin/gamma-secretase and regulates neural cell adhesion, cell migration, and neurite outgrowth. Mol Cell Biol. 2005;25:9040–53. [PubMed: 16199880]

[24]. Joubert F, Acosta MDC, Gallar J, Fakih D, Sahel JA, Baudouin C, et al. Effects of corneal injury on ciliary nerve fibre activity and corneal nociception in mice: A behavioural and electrophysiological study. Eur J Pain. 2019;23:589–602. [PubMed: 30370980]

Highlights:

Here we show that enucleation of eyes by cutting them out using curved scissors improves intraepithelial corneal nerve density and nerve terminal morphology compared to enucleation by pulling the eyes out and reduces variation between individual corneas.

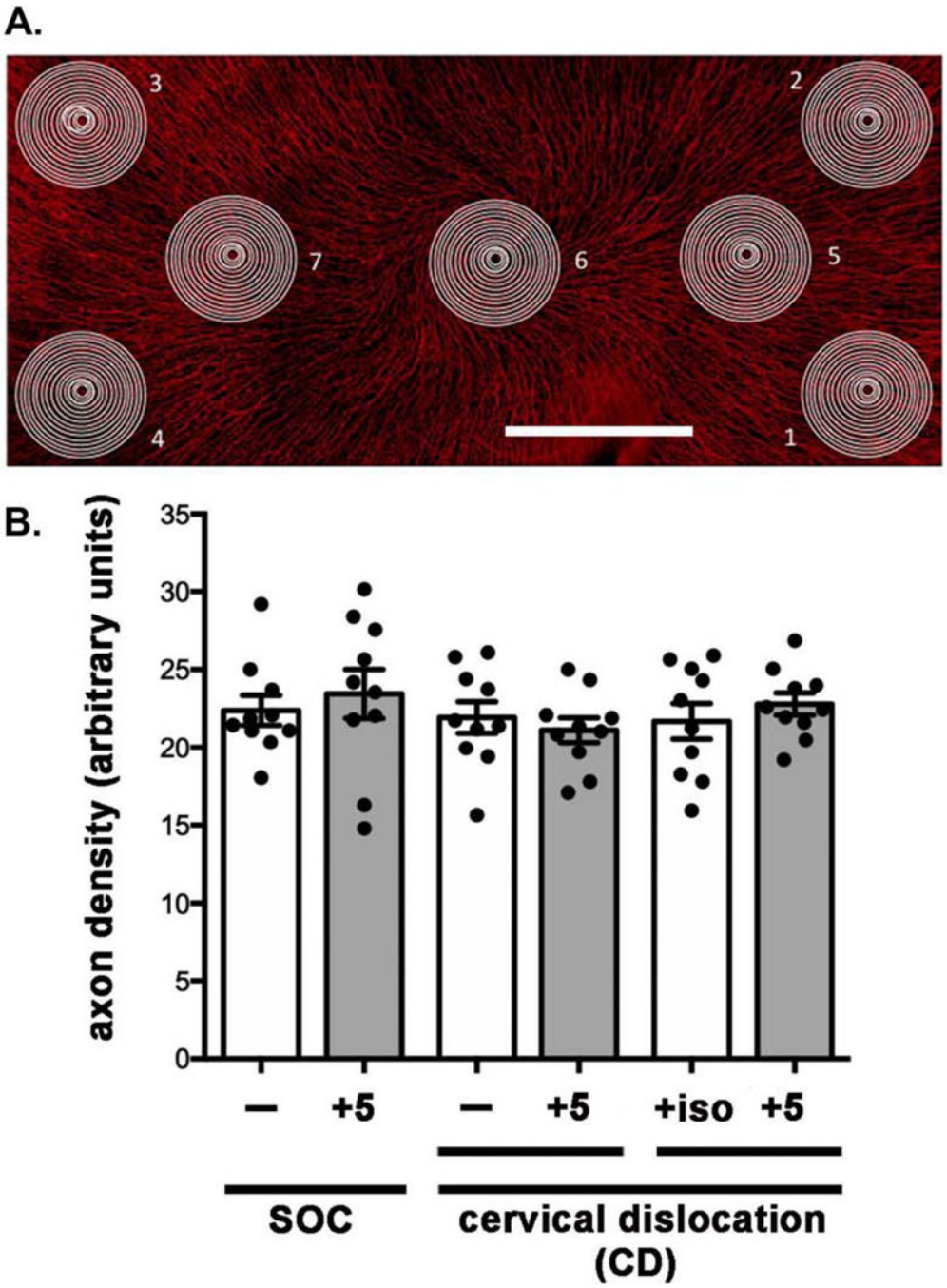

Figure 1. Cervical dislocation and delayed fixation by 5 min after euthanasia do not impact intraepithelial corneal nerve density (ICNs).

A. A representative en face image of a flat mounted mouse cornea stained to visualize the ICNs is shown. Axon density is assessed by Sholl analysis by placing targets at 7 sites: four at the corneal periphery and 3 at the corneal center. Bar = 500 μm. **B.** Axon density was assessed by Sholl analysis and the means and standard error of the means assessed for 10 corneas. Our standard of care (SOC, CO2 gas) was compared to cervical dislocation (CD) alone and CD after isoflurane gas to anesthetize mice (ISO). In addition, we determined

whether delaying enucleation for 5 minutes followed by fixation of the eyes after SOC euthanasia or CD impacts axon density. No significant differences were observed.

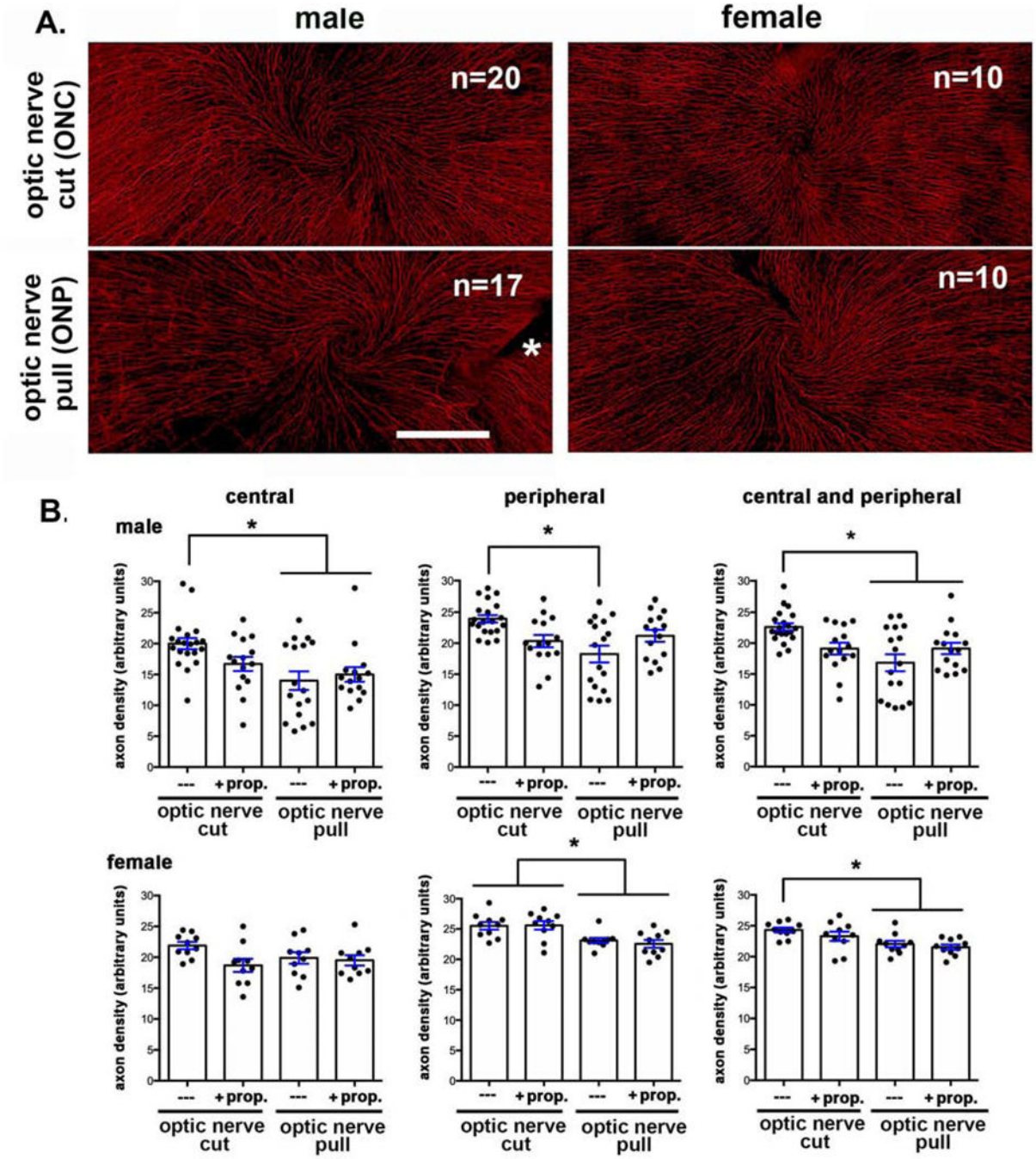

Figure 2. Enucleating eyes using the ONP method reduces ICN density compared to ONC where eyes are removed by cutting them out with curved scissors.

A. Representative en face images of flat mounted mouse corneas stained to visualize the ICNs are shown for each variable assessed. The asterisk indicates where an incision was made to flatten the cornea. Bar = 500 μm. **B.** Quantification shows significantly reduced axon density in male mice at the center, periphery and overall. While female mice also show reduced overall axon density, the reduction is less than that seen in the male mice and is more pronounced at the corneal periphery compared to the center.

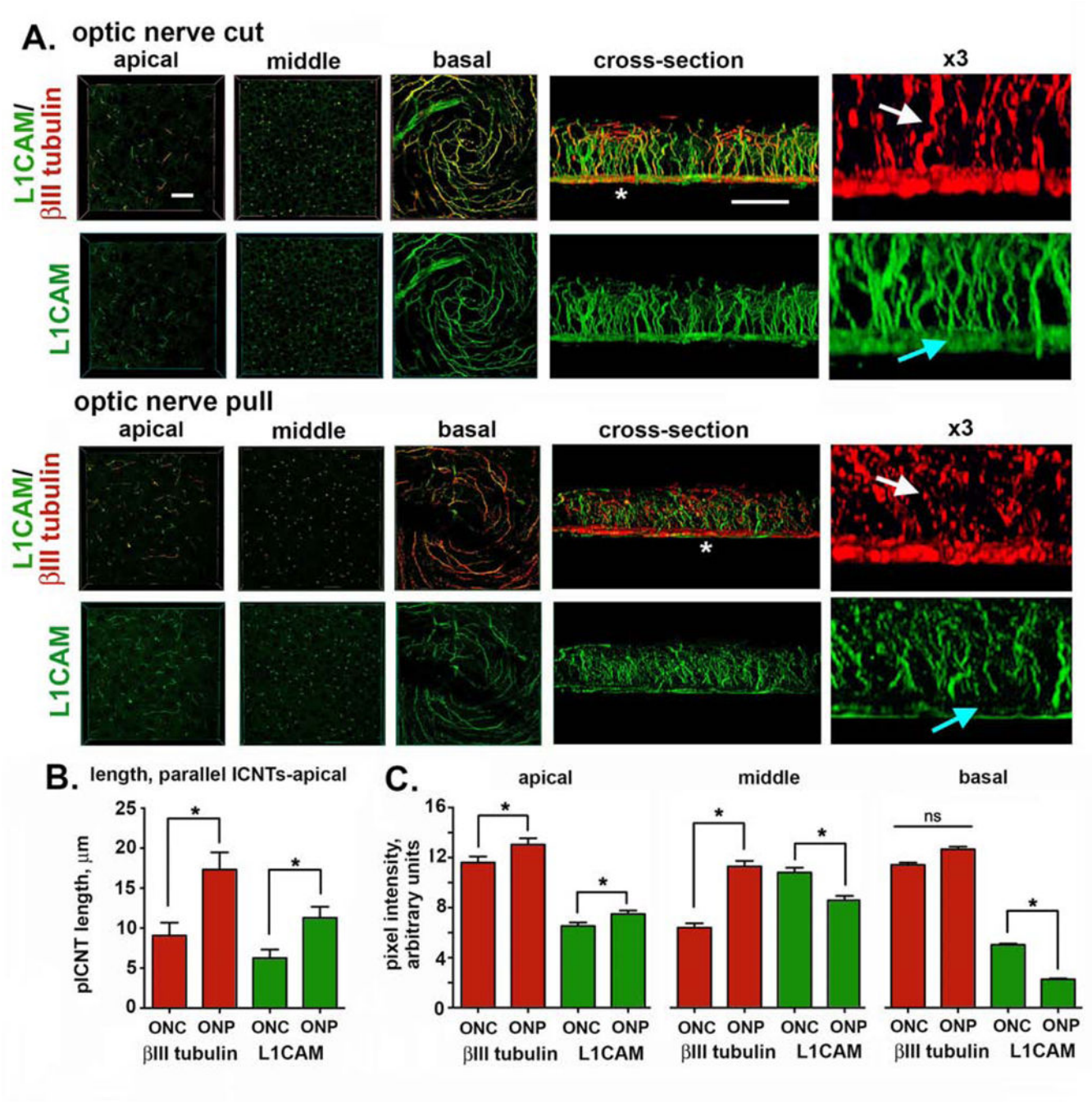

Figure 3. Enucleating eyes using the ONP method impacts ICNTs morphology and leads to shedding of L1CAM from the ICNTs.

A. High resolution confocal imaging was performed on mouse corneas enucleated using ONC or ONP after staining corneas to reveal the localization of L1CAM (green) and βIII tubulin (red). Representative en face images obtained through the apical, middle, and basal layers of the corneal epithelium are presented. 3D confocal image stacks were also obtained and rotated to allow cross-sectional view; representative cross section images are also shown. The sites indicated by the asterisks in the cross-sectional images were enlarged 3-fold and presented at the far right. White arrows show the ICNTs and highlight their beaded

morphology after ONP compared to ONC. Blue arrows indicate the reduction in L1CAM at the basal aspect of the corneal epithelium where the βIII-tubulin positive ICBNs are located. Bar in the en face images = 27 μm; bar in the cross-sectional images = 25 μm. **B.** The average lengths of the parallel ICNTs at the apical aspect of the corneal epithelium were measured using Image J. Data show that pICNTs are longer and retain L1CAM on their surface after ONP compared to ONC. **C.** Cross-sectional images were used to quantify L1CAM and βIII tubulin in the apical, middle, and basal regions of the corneal epithelium. Data show that ONP significantly reduces L1CAM retention on the ICBNs and the ICNTs in the middle of the corneal epithelium but does not impact the apical -most ICNTs.

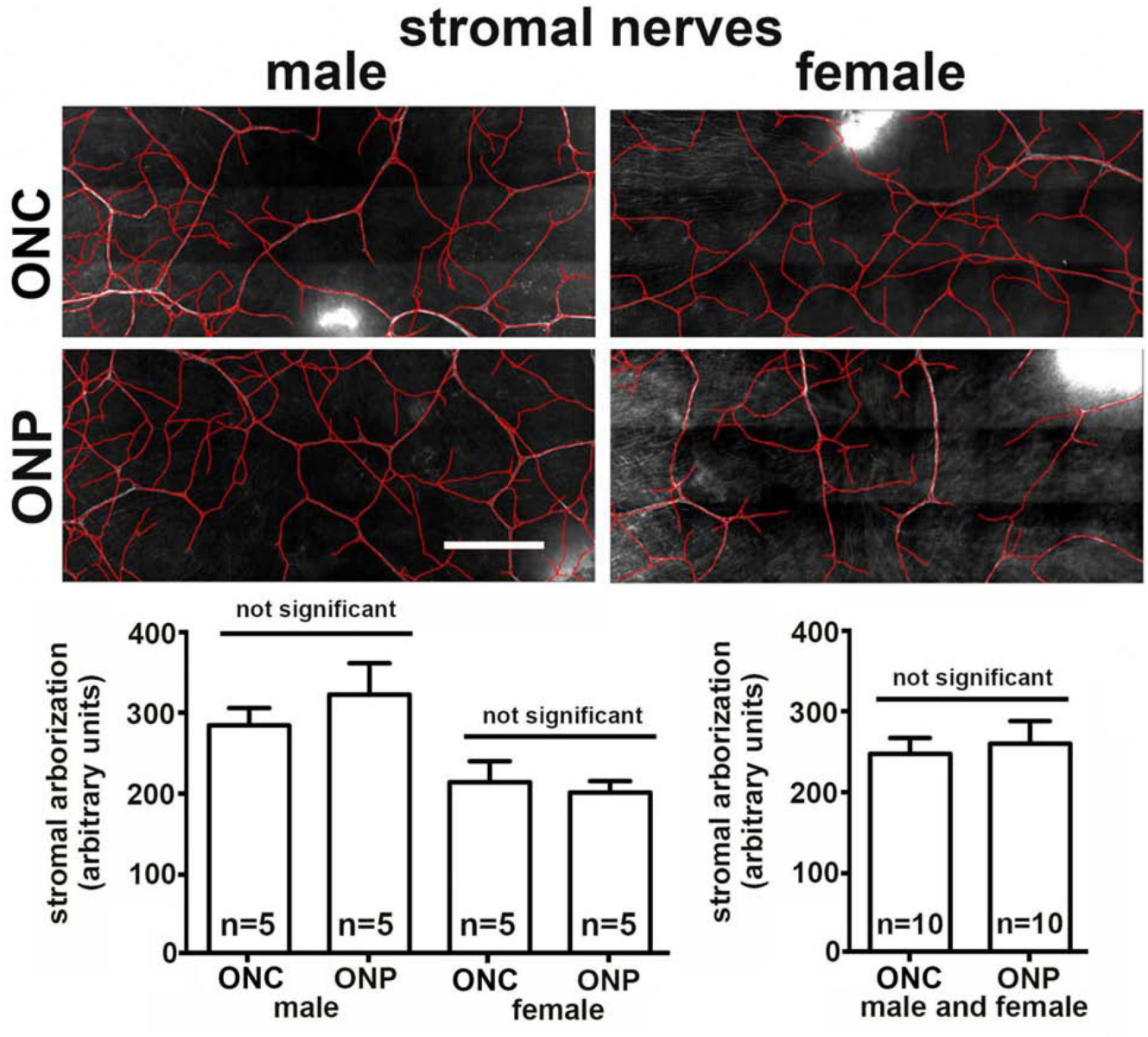

Figure 4. Enucleating eyes using the ONP method does not impacts stromal nerve arborization.

Shown are representative images of the corneal stromal nerves revealed by staining the corneas with antibodies against βIII tubulin after ONC and ONP. While male corneas showed a higher level of stromal nerve arborization compared to females, there are no significant differences induced by ONP. Bar = 500 μm.

Table 1.

The cornea as an independent variable. A Axon density (arbitrary units) B. Cell proliferation (ki67+ cells/fields) Table 1a is content under Sholl. Table 1b is content under ki67

Sholl

	mouse #	Left	Right	L+R/2	cage 1	cage 2
cage 1	1	14.1	21.7	17.9	14.1	21.1
	2	18.8	15.7	17.2	18.8	21.6
	3	22.0	15.4	18.7	22.0	21.9
	4	28.5	18.9	23.7	28.5	23.5
	5	24.3	23.6	23.9	24.3	---
cage 2	1	21.1	21.5	21.3	21.7	21.5
	2	21.6	15.1	18.4	15.7	15.1
	3	21.9	20.4	21.1	15.4	20.4
	4	23.5	17.7	20.6	18.9	17.7
	5	---	23.3	---	23.6	23.3
	n:	9	10	9	10	9
	mean:	21.8	19.3	20.3	20.3	20.7
	SD:	3.9	3.2	2.5	4.6	2.7
	SEM:	1.3	1	0.8	1.4	0.9

ki67

	mouse #	Left	Right	L+R/2	cage 1	cage 2
cage 1	1	327	313	320	327	247
	2	319	363	341	319	232
	3	291	210	250	291	181
	4	256	304	280	256	271
	5	262	296	279	262	---
cage 2	1	247	249	248	313	249
	2	232	275	253	363	275
	3	181	242	211	210	242
	4	271	232	251	304	232
	5	---	218	---	296	218
	n:	9	10	9	10	9
	mean:	265	270	271	294	238
	SD:	45	49	40	43	28
	SEM:	15	15	13	14	9